doi:10.1016/j.ijrobp.2009.01.031

PHYSICS CONTRIBUTION

INTEGRATION OF REAL-TIME INTERNAL ELECTROMAGNETIC POSITION MONITORING COUPLED WITH DYNAMIC MULTILEAF COLLIMATOR TRACKING: AN INTENSITY-MODULATED RADIATION THERAPY FEASIBILITY STUDY

RYAN L. SMITH,* AMIT SAWANT, PH.D.,[†] LAKSHMI SANTANAM, PH.D.,* RAGHU B. VENKAT, MS.,[†]
LAURENCE J. NEWELL, MS.,[‡] BYUNG-CHUL CHO, PH.D.,[†] PER POULSEN, PH.D.,[†] HERBERT CATELL,[§]
PAUL J. KEALL, PH.D.,[†] AND PARAG J. PARIKH, MD.*

*Washington University Saint Louis, Saint Louis, MO; [†]Stanford University, Palo Alto, CA; [‡]Calypso® Medical Technologies, Inc.,
Seattle, WA; and [§]Varian Medical Systems, Palo Alto, CA

Purpose: Continuous tumor position measurement coupled with a tumor tracking system would result in a highly accurate radiation therapy system. Previous internal position monitoring systems have been limited by fluoroscopic radiation dose and low delivery efficiency. We aimed to incorporate a continuous, electromagnetic, three-dimensional position tracking system (Calypso 4D Localization System) with a dynamic multileaf collimator (DMLC)–based dose delivery system.

Methods and Materials: A research version of the Calypso System provided real-time position of three Beacon transponders. These real-time three-dimensional positions were sent to research MLC controller with a motion-tracking algorithm that changed the planned leaf sequence. Electromagnetic transponders were embedded in a solid water film phantom that moved with patient lung trajectories while being irradiated with two different plans: a step-and-shoot intensity-modulated radiation therapy (S-IMRT) field and a dynamic IMRT (D-IMRT) field. Dosimetric results were recorded under three conditions: no intervention, DMLC tracking, and a spatial gating system.

Results: Dosimetric accuracy was comparable for gating and DMLC tracking. Failure rates for gating/DMLC tracking are as follows: ±3 cGy 10.9/ 7.5% for S-IMRT, 3.3/7.2% for D-IMRT; gamma (3mm/3%) 0.2/1.2% for S-IMRT, 0.2/0.2% for D-IMRT. DMLC tracking proved to be as efficient as standard delivery, with a two- to five-fold efficiency increase over gating.

Conclusions: Real-time target position information was successfully integrated into a DMLC effector system to modify dose delivery. Experimental results show both comparable dosimetric accuracy as well as improved efficiency compared with spatial gating.   © 2009 Elsevier Inc.

Radiation therapy, Intensity modulation, Lung, Cancer, DMLC, Tracking.

INTRODUCTION

Intensity-modulated radiation therapy (IMRT) is a widely used technique for delivering highly conformal radiation dose to a variety of tumor sites. The IMRT technique allows more accurate dose coverage and has been shown to improve clinical results in the prostate (1) as well as head and neck regions (2, 3). More recent efforts have focused on implementing IMRT delivery in the lung to limit the morbidity to healthy tissue (4).

Motion related to respiration, cardiac function, and the digestive system can all cause substantial tumor motion. Intrafraction motion is well documented to be problematic for radiation delivery to tumors in the abdomen, prostate (5), and thorax (6, 7). It has been shown via modeling (8) as well as experimentally (9) and clinically (10) that intrafraction motion can negate the benefits of using IMRT for delivering highly conformal dose gradients and therefore limit dose escalation because of unintentional irradiation of healthy tissue (11). Effectively managing intrafraction motion has led

---

to development of radiation delivery techniques such as breath hold techniques (12–16), respiratory gating (17–22), manual beam gating, and four-dimensional (4D) planning/tracking (23–28).

Breath hold techniques and coached breathing have been implemented for treatment planning, imaging, and dose delivery. These works show promise for spatial localization of internal structures. However many patients with lung cancer are unable to perform the required regular breathing throughout treatment (19).

Respiratory gating conventionally relies on the use of an external surrogate to correlate volumetric imaging with a specific phase of respiration. When the target leaves a predetermined volume, the accelerator is ''gated'' and the beam is shut off until the target re-enters the volume. There is an inherent tradeoff between spatial accuracy and delivery efficiency. Decreasing the gating volume will lead to very precise dose delivery, but the duty cycle for the system will fall dramatically and treatment times will increase. Aside from patient throughput, increased treatment times can have dosimetric consequences, as the patient is more likely to move if the treatment times increase (29). Another potential limitation of gating is that if the tumor moves outside of the gating volume for an extended period (*i.e.,* because of a non–respiratory-related shift in the patient), the gating system cannot account for this, and the treatment will pause until the patient is manually readjusted.

An ideal motion compensation solution would offer both dosimetric accuracy and efficient, flexible delivery. Here, we propose a solution using a dynamic multileaf collimator (DMLC) to track moving treatment targets. This system has the potential for delivering highly conformal and accurate IMRT treatments in an efficient manner.

To use DMLC tracking as an effector system, it is necessary to obtain accurate real-time low-latency information on the tumor position throughout the course of treatment. Although it has been shown that, for respiratory-related motion, correlation exists between the movements of external anatomy and internal tumor motion (28, 30), in some cases this correlation breaks down (31). Preferably, tumor positions would be continuously measured internally without the use of ionizing radiation, thus eliminating problems associated with changes in the relationship between the tumor and the position monitoring system without additional imaging dose to the patient.

Here we report the use of an electromagnetic position monitoring solution integrated with a DMLC effector system. We use a research version of the Calypso 4D Localization System (Calypso Medical, Seattle, WA) that provides real-time position monitoring of up to three internal fiducial transponders without the use of ionizing radiation. In a related study, we investigated the geometric accuracy of the combined system by measuring the ability of the system to center a circular aperture in response to motion. We have demonstrated that the system can ''move'' the treatment beam to compensate for target motion (32) with a mean geometric accuracy of 1.42 mm RMSE in the leaf direction and 0.60 mm RMSE orthog-
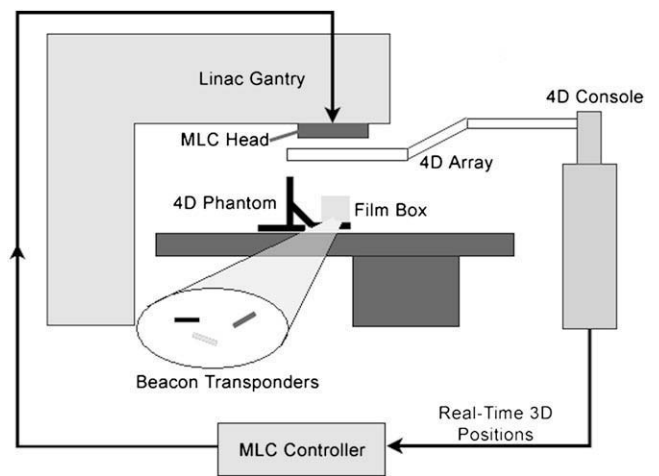
Fig. 1. Four-dimensional (4D) phantom motion stage moves a film box containing dosimetric film. Three electromagnetic transponders are embedded in the film box provide real-time position output to a computer controlling the multileaf collimator (MLC) leaves. Leaf positions are updated to follow the motion of the target. 3D = three-dimensional.

onal to the leaf direction when tracking a human patient–derived lung trajectory.

Even with known geometric accuracy of the system, there remain clinical questions regarding implementation. Interplay between the IMRT delivery technique and tumor motion can lead to dosimetric error (9, 33–35). Moreover, the addition of a motion tracking system to MLC movement during delivery adds complexity to the therapy quality assurance. Our hypothesis was that an integrated electromagnetic position measurement–DMLC tracking system should show similar dosimetric results to an electromagnetic position measurement–gating system, but with improved efficiency.

METHODS AND MATERIALS

Experimental setup

A schematic diagram of the setup is shown in Fig. 1. A research version of the Calypso System provided real-time position data output of three Beacon electromagnetic transponders at an acquisition frequency of 25 Hz. This data stream containing 3D position information of the tracked centroid was sent to two effector systems. The first system used spatial gating and has been described previously (36). Spatial gating using electromagnetic transponders uses real-time internal position monitoring. The real-time 3D position of the implanted fiducials is compared with a predefined 3D volume. If the position is within the 3D volume, treatment commences. If the target leaves the volume, a BEAM_HOLD is enacted at the linear accelerator until the target returns and the real-time position is within the volume. In these experiments, the gating system received the 3D position and compared it with a predetermined 4 × 4 × 4-mm spatial volume.

The second effector system was the DMLC tracking system (37). The 3D position was input to a research MLC controller with a modified linear adaptive motion tracking algorithm (38). The algorithm altered the planned leaf sequence based on the real-time 3D position data and sent new leaf positions to the Millenium MLC controller on a Varian Trilogy (Varian Medical Systems, Palo Alto, CA) at 20 Hz.

(A) Step and Shoot Films
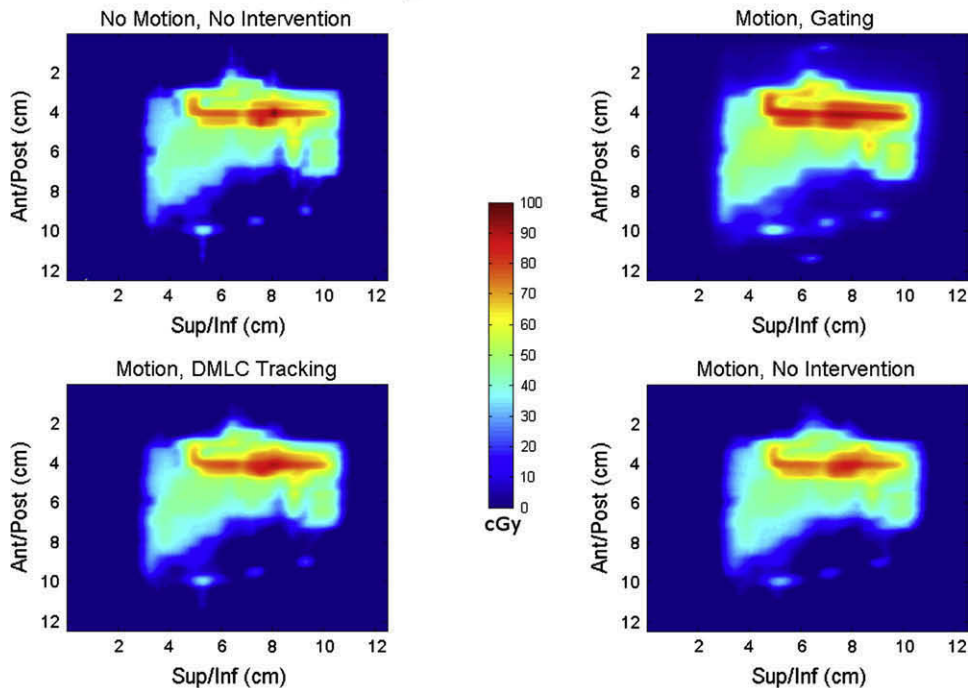
(B) D-IMRT Films
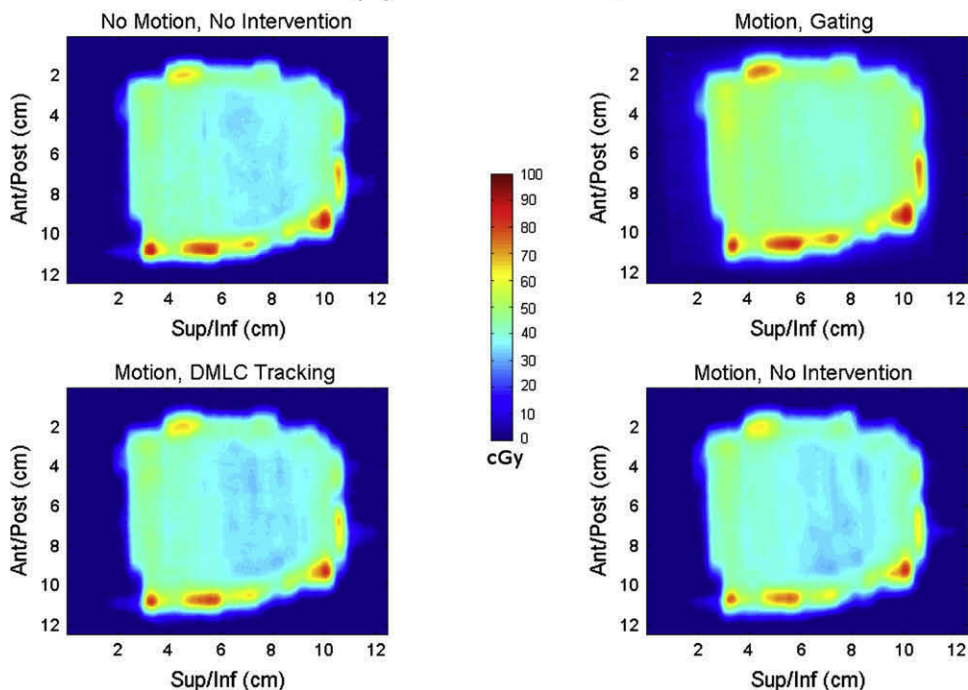
Fig. 2. Dosimetric films were aligned at isocenter in the sagittal plane were used to observe the delivered dose. Intensity-modulated radiation therapy (IMRT) plans were delivered via step and shoot (A) and dynamic IMRT (D-IMRT) (B) delivery methods in the following scenarios: no motion, motion with no intervention, motion with dynamic multileaf collimator tracking, and motion with a 4-mm gating window. Sup/inf = superior/inferior.

The prediction time for the algorithm was set at 220 ms based on previous latency estimates calculated for the system (32). Beacon electromagnetic transponders (Calypso Medical Technologies, Inc., Seattle, WA) were embedded in a solid water phantom along with dosimetric film (Kodak EDR2) located in the sagittal plane aligned at isocenter. The entire film box was placed on the Washing-ton University 4D Phantom, a motion platform capable of recreating patient breathing trajectories to submillimeter accuracy (39).

The following settings were used for all cases: gantry 90°, colli-mator 90°, and 200 MU delivered via a 6-MV photon beam. The MLC leaves for both the S-IMRT and D-IMRT plans were aligned in the superior/inferior (primary) direction of motion. The delivered

(A) Step and Shoot

(B) D-IMRT
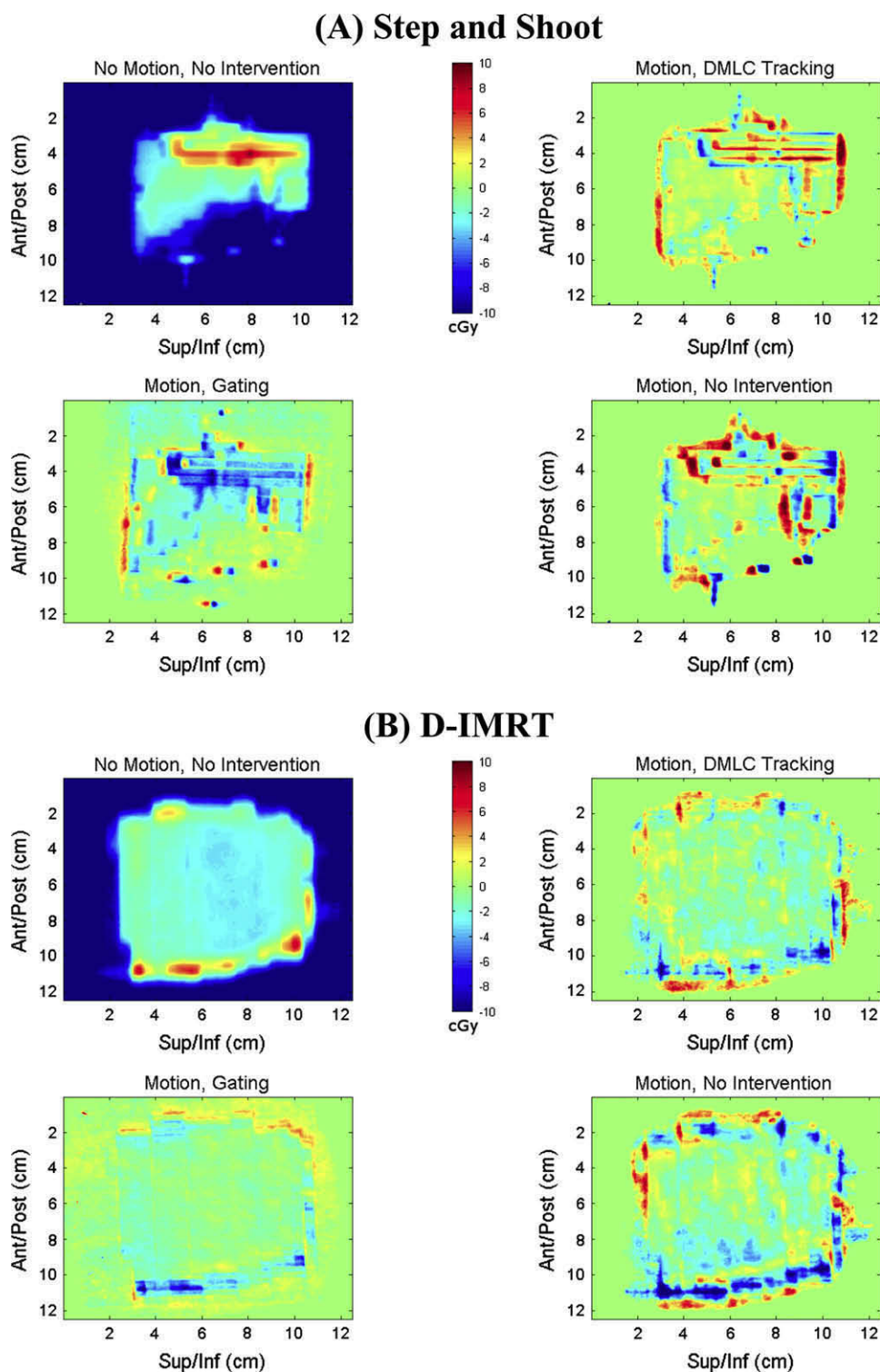
Fig. 3. Difference maps were produced after registering dose profiles in the presence of motion with film obtained via static delivery (the "gold standard"). Control is given as reference in each case. Sup/inf = superior/inferior.

dose for each plan was approximately 100 cGy at isocenter. The moving phantom was loaded with a single film aligned in the sagittal plane at isocenter and irradiated as it moved with two different plans: (*1*) an S-IMRT field, and (*2*) a D-IMRT field. The phantom was programmed with no motion or with motion obtained from a lung cancer patient using the CyberKnife Synchrony (Accuray, Sunnyvale, CA) tracking system (40). The trajectory had a frequency

of 23 breaths/min and had the following peak-to-peak amplitudes: 7 mm lateral, 23 mm superior/inferior, and 6 mm anterior/posterior. The breathing trajectory was relatively periodic, however, and not totally uniform throughout the treatment. Dosimetric results in the presence of motion were recorded for each plan using three different effector systems: no intervention, DMLC tracking, and a $4 \times 4 \times 4$-mm spatial gating system. The comparators for the dosimetric

results in the presence of motion were the dose results obtained with a static target.

The films in the presence of motion were registered to the static delivery case in the absence of motion. Once registered, the difference maps were calculated to determine the level of under- or overdosing.

Gamma analysis

Difference maps tend to break down in regions of high dose gradient because a small spatial offset can provide a relatively large dose difference. Conventionally, distance to agreement maps are complementary to difference maps in the sense that they work well in regions of high dose gradient and exhibit high dissimilarity for relatively low dosimetric differences in regions of low gradient. Here, we use the γ tool to evaluate each measurement (41). The γ tool effectively combines both dose difference and distance to agreement metrics which each break down in steep and shallow dose gradient regions respectively. The γ function is defined as the minimum generalized gamma function for all points:

$$\Gamma\left(\overrightarrow{r_e}, \overrightarrow{r_r}\right) = \sqrt{\frac{r^2\left(\overrightarrow{r_e}, \overrightarrow{r_r}\right)}{\Delta d^2} + \frac{\delta^2\left(\overrightarrow{r_e}, \overrightarrow{r_r}\right)}{\Delta D^2}} \Bigg| \text{ Generalized } \Gamma \text{ function.}$$

Where $\overrightarrow{r_e}$, $\overrightarrow{r_r}$ are the positions on the evaluated and reference images respectively, $r(\overrightarrow{r_e}, \overrightarrow{r_r})$ is the spatial distance between the two points, $\delta^2(\overrightarrow{r_e}, \overrightarrow{r_r})$ is the difference between the evaluated dose and the reference dose at their respective positions, Δd is the distance to agreement criterion (here, 3 mm), and ΔD is the dose agreement criterion (here, 3% of the maximum dose). We leave out the details for the sake of brevity; however, further information on the γ tool can be found in the literature (41).

Efficiencies

In addition to dosimetric accuracy, the delivery efficiencies were recorded for each case. The ''Beam-On Time'' and ''Total Time'' displayed on the console of the Linac were recorded for each delivery. These metrics are used to determine the efficiency of delivery for each effector system. Delivery without intervention requires Beam Holds as the leaves in the MLC move from position to position. Our metric for efficiency uses a normalized duty cycle in which 100% matches the efficiency of delivery without intervention.

RESULTS

Dosimetry

Figure 2 displays the raw films for each delivery case. Dose blurring is evident for the film irradiated in the presence of motion with no intervention. Gating and DMLC tracking significantly reduce the dosimetric artifacts associated with irradiating a moving target. For all dosimetric analysis, the static film irradiated in the absence of motion serves as the control.

Figure 3 shows the dose difference maps between each of the effector systems and the static ''gold standard'' film. For the S-IMRT case (Fig. 3A), the DMLC tracking difference map and gating difference map show similar amounts of mismatch, although the locations of the mismatch differ.

For the single field D-IMRT difference maps (Fig. 3B), the gating and DMLC tracking films are comparable. The dose in the interior of the region is relatively homogeneous, and as

Table 1. Dosimetry failure rates for two types of intensity-modulated radiation therapy (IMRT) plan

Plan	Intervention	3%, 3 mm	6%, 6 mm	±3 cGy	±5 cGy
S-IMRT	Gating	0.18%	0.00%	10.91%	3.26%
S-IMRT	DMLC	1.21%	0.00%	7.53%	2.73%
S-IMRT	None	2.45%	0.16%	10.86%	5.02%
D-IMRT	Gating	0.22%	0.00%	3.30%	0.64%
D-IMRT	DMLC	0.24%	0.20%	7.20%	2.02%
D-IMRT	None	1.55%	1.09%	13.06%	4.99%

Abbreviations: D-IMRT = dynamic IMRT; S-IMRT = step-and-shoot IMRT.

Note: Gamma failure rates were reported for all cases. Failure rates for D-IMRT plans were comparable for gating and DMLC tracking. S-IMRT gating outperformed DMLC tracking. Gating and DMLC tracking outperformed no intervention in both plans.

a result a difference map is not the best metric for observing dose artifacts caused by motion.

In the S-IMRT delivery, the percentage of points with a difference of ±3 cGy from the static case were 10.91% and 7.53% for gating and DMLC tracking, respectively; for the D-IMRT, 3.30% failed for gating, whereas 7.20% failed for DMLC tracking (Table 1).

Analysis of the gamma output for 3 mm and 3% shows that gating outperforms DMLC tracking for the S-IMRT case, with failure rates of 0.18% and 1.21%, respectively (Fig. 4). For the D-IMRT case, the two intervention methods were comparable, with failure rates of 0.22% for gating and 0.24% for DMLC tracking (Table 1). Both methods of intervention outperform no intervention, which produced failure rates of 2.45% and 1.45% in the presence of motion for the S-IMRT and the D-IMRT plan.

Efficiency

The study results show that DMLC tracking allows drastic improvement in delivery efficiency when compared with beam gating (Table 2). The DMLC tracking showed no decrease in efficiency for both S-IMRT and D-IMRT plans (100% efficiency). Beam gating exhibited efficiency values of 38% for the S-IMRT plan and 22% for the D-IMRT plan.

DISCUSSION

We have successfully implemented a tracking system that does not rely on ionizing radiation or an external tumor surrogate for the detection of internal targets. The DMLC tracking solution shows promise for the reduction of motion-related dosimetric errors. However there are several details that still need to be addressed.

For the case of the D-IMRT plan, the gating solution produced comparable dosimetric output when compared with the DMLC tracking. The D-IMRT plan shows relatively few high dose gradient regions in the center of the dose distribution. As a result, in the interior of the target, the dosimetric errors associated with superior inferior motion are not as evident from a difference map.
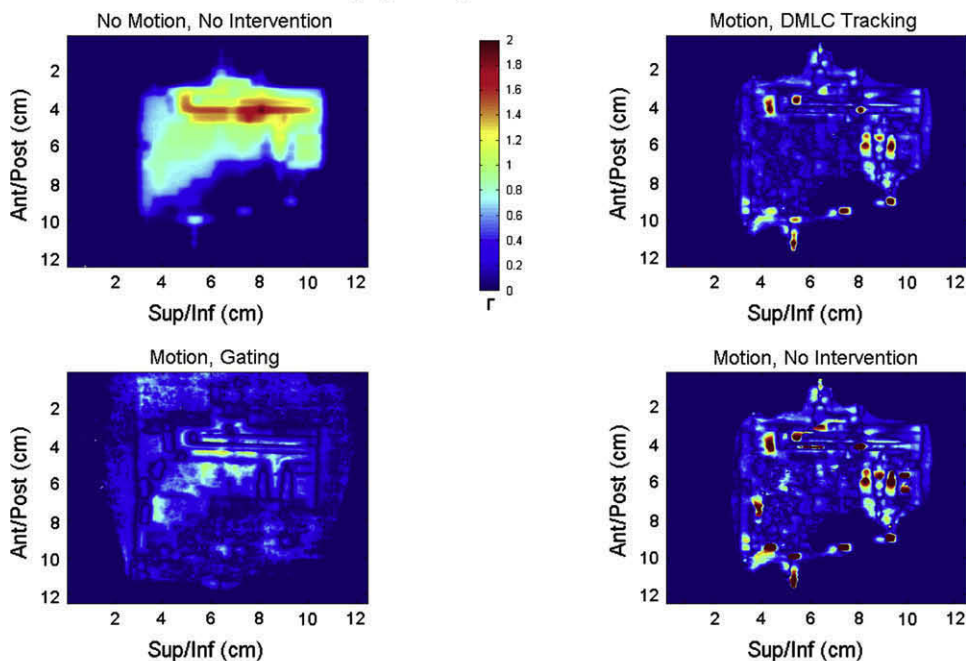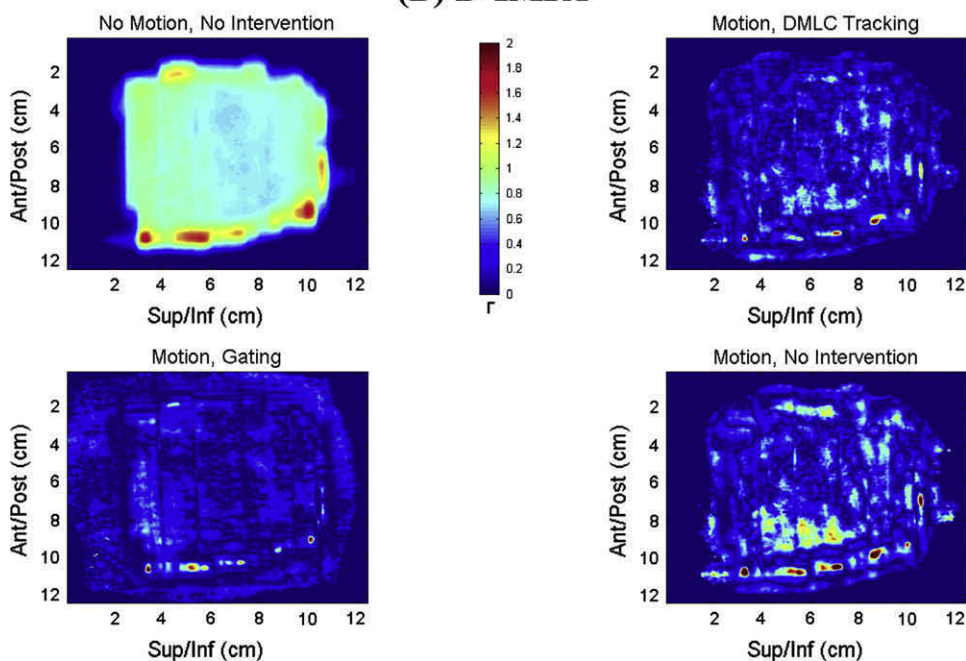
Fig. 4. Gamma values were calculated for each of moving image. Values for distance to agreement criterion $\Delta d = 3$ mm and dose agreement criterion $\Delta D = 3\%$ of maximum dose. Control is given as reference for each case. Sup/inf = superior/inferior.

The S-IMRT delivery to the moving phantom with no intervention corresponds to a convolution of the beam profile for each step-and-shoot segment with the motion of the phantom during delivery of that segment. With gating, the delivery corresponds to a convolution with the residual motion within the gating window. Therefore, one would expect small blurring of the dose profiles with dosimetric errors related to the size of the gating volume. The errors associated with

DMLC tracking are not as clear. Here, the discrepancy with the static case is caused by failure to align instantaneously to the target position and the coarse (one-leaf width) aperture resolution orthogonal to the leaf direction. It is possible that the target motion oscillated in a fashion that dictated a shift back and forth of one leaf position in the anterior/posterior direction; this could lead to substantial dosimetric error on the order of the size of the one leaf (5 mm). It should be noted that

Table 2. Efficiency values for two types of intensity-modulated radiation therapy (IMRT) plan

Plan	Intervention	Beam on time (min)	Total time (min)	Duty cycle (normalized)
S-IMRT	None	0.32	0.64	100%
S-IMRT	DMLC	0.32	0.60	100%
S-IMRT	Gating	0.30	1.68	38%
D-IMRT	None	0.33	0.35	100%
D-IMRT	DMLC	0.32	0.36	100%
D-IMRT	Gating	0.30	1.53	22%

Abbreviations: D-IMRT = dynamic IMRT; S-IMRT = step-and-shoot IMRT.

Note: Delivery efficiencies were recorded in the form of beam on time and total time for each of the delivery conditions. Values along with associated duty cycles are displayed. Duty cycle values are normalized to the static delivery case (100% indicates no efficiency drop caused by intervention).

our algorithm did not use subleaves to estimate motion orthogonal to the leaf direction (37). As a result, a shift in the anterior/posterior direction is "all or nothing," which could potentially have led to the dosimetric error seen in the S-IMRT DMLC tracking films.

It is notable that increased efficiency has potential for dosimetric implications, not just patient throughput. If the patient is on the table for a considerably greater duration (*i.e.,* using a gating solution with a very small gating window), it is possible the patient will move because of discomfort. Although not in the scope of this experiment, this motion has potential dosimetric consequences.

There is further work to be done on the system. Currently there is variable latency in the position monitoring which is not taken into account by the prediction algorithm. Setting a fixed latency for the position monitoring, or accounting for the variable latency in the MLC tracking algorithm would provide for better geometric (and hence dosimetric) results. In addition, reducing the overall latency of the system as

a whole would provide for better dosimetric results. Incorporating target deformation and rotation into the beam shaping is another potential improvement for the system. Work needs to be done to evaluate a variety of treatment plans to ensure that the MLC tracking algorithm is robust and accurate when applied to any conventionally generated treatment plan.

There are plans for commercialization of this system. It may be safer to implement the system for prostate cancer management, as there are currently approved uses for Calypso Beacon implantation for that location. Further uses, such as lung tumor tracking, will need a new transponder design that can be safely inserted in the thorax. It is not clear whether changes in treatment planning software will be necessary, although they may be desirable to fully take advantage of the DMLC tracking capability. The tools for quality assurance of the system will have to be developed and may include motion phantoms such as the one used in this work. Safety and reliability of a commercial implementation will have to be investigated in a more thorough manner than in this preliminary work.

CONCLUSION

In summary, we have integrated a system that senses real-time internal anatomy positions without the use of ionizing radiation with a DMLC tracking system to deliver continuous dose to a moving target. The dose profiles are comparable with an idealized gating algorithm, eliminate the uncertainties inherent in the use of chest wall surrogates for tumor position, and show much higher delivery efficiencies as well as the promise of increased clinical confidence of the radiation dose delivery to the treatment target during radiation delivery. More work is left to be done in further improving the dosimetric results in an effort to create a system that delivers accurate radiation with submillimeter intrafraction motion management.

REFERENCES

1. Zelefsky MJ, Fuks Z, Happersett L, *et al*. Clinical experience with intensity modulated radiation therapy (IMRT) in prostate cancer. *Radiother Oncol* 2000;55:241–249.
2. Ozyigit G, Yang T, Chao KSC, *et al*. Intensity-modulated radiation therapy in head and neck cancers: The Mallinckrodt experience. *Curr Treat Options in Oncol* 2004;5:3–9.
3. Münter MW, Thilmann C, Hof H, *et al*. Stereotactic intensity modulated radiation therapy and inverse treatment planning for tumors of the head and neck region: Clinical implementation of the step and shoot approach and first clinical results. *Radiother Oncol* 2003;66:313–321.
4. Grills IS, Yan D, Martinez AA, *et al*. Potential for reduced toxicity and dose escalation in the treatment of inoperable non–small-cell lung cancer: A comparison of intensity-modulated radiation therapy (IMRT), 3D conformal radiation, and elective nodal irradiation. *Int J Radiat Oncol Biol Phys* 2003; 57:875–890.
5. Kupelian P, Willoughby T, Mahadevan A, *et al*. Multi-institutional clinical experience with the Calypso System in localization and continuous, real-time monitoring of the prostate

gland during external radiotherapy. *Int J Radiat Oncol Biol Phys* 2007;67:1088–1098.
6. George R, Keall PJ, Kini VR, *et al*. Quantifying the effect of intrafraction motion during breast IMRT planning and dose delivery. *Med Phys* 2003;30:552–562.
7. Langen KM, Jones DT. Organ motion and its management. *Int J Radiat Oncol Biol Phys* 2001;50:265–278.
8. Bortfeld T, Jokivarsi K, Goitein M, *et al*. Effects of intrafraction motion on IMRT dose delivery: Statistical analysis and simulation. *Phys Med Biol* 2002;47:2203–2220.
9. Jiang SB, Pope C, Jarrah KMA, *et al*. An experimental investigation on intra-fractional organ motion effects in lung IMRT treatments. *Phys Med Biol* 2003;48:1773–1784.
10. Gierga DP, Chen GTY, Kung JH, *et al*. Quantification of respiration-induced abdominal tumor motion and its impact on IMRT dose distributions. *Int J Radiat Oncol Biol Phys* 2004; 58:1584–1595.
11. Marnitz S, Stuschke M, Bohsung J, *et al*. Intraindividual comparison of conventional three-dimensional radiotherapy and intensity modulated radiotherapy in the therapy of locally

advanced non-small cell lung cancer. *Strahlenther Onkol* 2002; 178:651–658.

12. Hanley J, Debois MM, Mah D, *et al.* Deep inspiration breath-hold technique for lung tumors: The potential value of target immobilization and reduced lung density in dose escalation. *Int J Radiat Oncol Biol Phys* 1999;45:603–611.

13. Rosenzweig KE, Hanley J, Mah D, *et al.* The deep inspiration breath-hold technique in the treatment of inoperable non-small-cell lung cancer. *Int J Radiat Oncol Biol Phys* 2000;48:81–87.

14. Barnes EA, Murray BR, Robinson DM, *et al.* Dosimetric evaluation of lung tumor immobilization using breath hold at deep inspiration. *Int J Radiat Oncol Biol Phys* 2001;50:1091–1098.

15. Balter JM, Lam KL, McGinn CJ, *et al.* Improvement of CT-based treatment-planning models of abdominal targets using static exhale imaging. *Int J Radiat Oncol Biol Phys* 1998;41:939–943.

16. Wong JW, Sharpe MB, Jaffray DA, *et al.* The use of active breathing control (ABC) to reduce margin for breathing motion. *Int J Radiat Oncol Biol Phys* 1999;44:911–919.

17. Shirato H, Shimizu S, Kunieda T, *et al.* Physical aspects of a real-time tumor-tracking system for gated radiotherapy. *Int J Radiat Oncol Biol Phys* 2000;48:1187–1195.

18. Kini VR, Vedam SS, Keall PJ, *et al.* Patient training in respiratory-gated radiotherapy. *Med Dosim* 2003;28:7–11.

19. Kubo HD, Len PM, Minohara S, *et al.* Breathing-synchronized radiotherapy program at the University of California Davis Cancer Center. *Med Phys* 2000;27:346–353.

20. Berson AM, Emery R, Rodriguez L, *et al.* Clinical experience using respiratory gated radiation therapy: Comparison of free-breathing and breath-hold techniques. *Int J Radiat Oncol Biol Phys* 2004;60:419–426.

21. Kubo HD, Hill BC. Respiration gated radiotherapy treatment: A technical study. *Phys Med Biol* 1996;41:83–91.

22. Ramsey CR, Scaperoth D, Arwood D, *et al.* Clinical efficacy of respiratory gated conformal radiation therapy. *Med Dosim* 1999;24:115–119.

23. Keall P. 4-Dimensional computed tomography imaging and treatment planning. *Semin Radiat Oncol* 2004;14:81–90.

24. Rietzel E, Chen GTY, Choi NC, *et al.* Four-dimensional image-based treatment planning: Target volume segmentation and dose calculation in the presence of respiratory motion. *Int J Radiat Oncol Biol Phys* 2005;61:1535–1550.

25. Keall PJ, Joshi S, Vedam SS, *et al.* Four-dimensional radiotherapy planning for DMLC-based respiratory motion tracking. *Med Phys* 2005;32:942–951.

26. Shirato H, Shimizu S, Kitamura K, *et al.* Four-dimensional treatment planning and fluoroscopic real-time tumor tracking radiotherapy for moving tumor. *Int J Radiat Oncol Biol Phys* 2000;48:435–442.

27. Adler JR Jr., Chang SD, Murphy MJ, *et al.* The Cyberknife: A frameless robotic system for radiosurgery. *Stereotact Funct Neurosurg* 1997;69:124–128.

28. Seppenwoolde Y, Berbeco RI, Nishioka S, *et al.* Accuracy of tumor motion compensation algorithm from a robotic respiratory tracking system: A simulation study. *Med Phys* 2007;34:2774–2784.

29. von Siebenthal M, Székely G, Lomax AJ, *et al.* Systematic errors in respiratory gating due to intrafraction deformations of the liver. *Med Phys* 2007;34:3620–3629.

30. Berbeco RI, Nishioka S, Shirato H, *et al.* Residual motion of lung tumours in gated radiotherapy with external respiratory surrogates. *Phys Med Biol* 2005;50:3655–3667.

31. Gierga DP, Brewer J, Sharp GC, *et al.* The correlation between internal and external markers for abdominal tumors: Implications for respiratory gating. *Int J Radiat Oncol Biol Phys* 2005;61:1551–1558.

32. Sawant A, Smith RL, Venkat RB. Geometric accuracy and latency of an integrated 4D IMRT delivery system using real-time internal position monitoring and dynamic MLC tracking. *Int J Radiat Oncol Biol Phys* 2008;72:S27–S28.

33. Verellen D, Tournel K, Van de Steene J, *et al.* Breathing-synchronized irradiation using stereoscopic kV-imaging to limit influence of interplay between leaf motion and organ motion in 3D-CRT and IMRT: Dosimetric verification and first clinical experience. *Int J Radiat Oncol Biol Phys* 2006;66:108–119.

34. Berbeco RI, Pope CJ, Jiang SB. Measurement of the interplay effect in lung IMRT treatment using EDR2 films. *J Appl Clin Med Phys* 2006;7:33–42.

35. Verellen D, Tournel K, Linthout N, *et al.* Importing measured field fluences into the treatment planning system to validate a breathing synchronized DMLC-IMRT irradiation technique. *Radiother Oncol* 2006;78:332–338.

36. Parikh P, Lechleiter K, Malinowski K, *et al.* Dosimetric effects of a 4D magnetic localization system for LINAC beam gating on prostate and lung radiation therapy. *Medical Physics* 2007;34:2625.

37. Sawant A, Venkat R, Srivastava V, *et al.* Management of three-dimensional intrafraction motion through real-time DMLC tracking. *Med Phys* 2008;35:2050–2061.

38. Srivastava V, Keall P, Sawant A, *et al.* Accurate prediction of intra-fraction motion using a modified linear adaptive filter. *Med Phys* 2007;34:2546.

39. Malinowski K, Lechleiter K, Hubenschmidt J. Use of the 4D phantom to test real-time targeted radiation. *Med Phys* 2007;34:2611.

40. Suh Y, Dieterich S, Cho B, *et al.* An analysis of thoracic and abdominal tumour motion for stereotactic body radiotherapy patients. *Phys Med Biol* 2008;53:3623–3640.

41. Low DA, Dempsey JF. Evaluation of the gamma dose distribution comparison method. *Med Phys* 2003;30:2455–2464.